Influence of Dopant Substitution Mechanism on Catalytic Properties within Hierarchical Architectures

Stephanie H. Newland,[1] Wharton Sinkler,[2] Thomas Mezza,[2] Simon R. Bare[2,3] and Robert Raja[1*]

[1]*School of Chemistry, University of Southampton, Southampton, SO17 1BJ, United Kingdom; R.Raja@soton.ac.uk;*
[2]*UOP LLC, a Honeywell Company, Des Plaines, Illinois 60017, United States*
[3] SSRL, SLAC National Accelerator Laboratory, Menlo Park CA, 94025, USA

Abstract:

A range of hierarchically porous AlPO-5 catalysts, with isomorphously substituted transition metal ions, have been synthesised using an organosilane as a soft template. By employing a range of structural and spectroscopic characterisation protocols, the properties of the dopant substituted species within the hierarchically porous architectures, has been carefully evaluated. The resulting nature of the active site is shown to have a direct impact on the ensuing catalytic properties in the liquid-phase Beckmann rearrangement of cyclic ketones.

Keywords: Hierarchically-Porous, Isomorphous-Substitution, Aluminophosphates, Beckmann Rearrangement, Active-site design

Introduction and design strategy

The rational design of isolated active centres within porous architectures affords a viable strategy for the production of sustainable catalysts. Precise design of discrete active centres is widely recognised as being the cornerstone in the development of a single-site heterogeneous catalyst (SSHC).(1) SSHC can be composed of isolated individual atoms or complexes, which are spatially-separated without interaction, so each active site will have an equivalent energetic interaction with incoming reagents. This results in the generation of highly active and selective active sites, which have proved effective for catalysing a wide-range of chemical transformations that have benefited both industry and society. (2-7)

Researchers have long explored the development of such isolated active sites through isomorphous substitution within aluminosilicates (zeolites) and aluminophosphates (AlPOs), since their conception in 1982.(8) The introduction of a range of transition-metal dopants was explored within zeolites for a wide-variety of oxidation and acid-catalysed transformations.(9-12) One of the most

striking examples was the discovery of titanosilicate-1 (TS-1), where isomorphous replacements of Si(IV) with small quantities (c.a. 2 atom percent) of tetrahedral Ti(IV) species, catalysed a range of industrially-significant, selective oxidation reactions (e.g. oxidation of benzene, phenol, epoxidation of propylene, etc), using hydrogen peroxide (H_2O_2) as the oxidant.(10, 13-16) Similarly, the introduction Fe(III) in MFI architectures (Fe-ZSM-5) proved effective in the singlet-oxygen catalysed oxidation of benzene to phenol, which was an important milestone in the C-H activation of hydrocarbons and aromatics.(2, 17, 18) AlPOs consist of repeating Al(III) and P(V) tetrahedra, and often form analogous frameworks to zeolites. The Al-O-P bonds in the AlPO architecture are more ionic in character than the bonds found within zeolites, and hence these materials are far more amenable to a wider-range of isomorphous substitution than zeolites. AlPOs, indeed, have proved themselves to be extremely compositionally diverse with more than 20 different transition-metals being substituted into the framework (in a tetrahedral geometry) with various oxidation states.(19, 20) Hence these frameworks have the potential to combine a specific coordination geometry, with isolated catalytically active sites, in order to create novel, robust, superior catalyst with high activities and selectivities.

There are three different substitution mechanisms available for isomorphous substitution (Figure 1) within AlPOs. The dopant oxidation state and the framework atom that is to be replaced determine the substitution mechanism followed. Dextrous choice of dopants can result in the creation of active sites within the AlPO catalysts, which are highly active for specific reactions. For example it is possible to create a Brønsted acid site within an AlPO framework through substituting Al(III) with Co (II), via type I substitution, which leads to the formation of negatively charged framework. During the synthesis the net negative charge will be quenched by a combination of structure directing agent (protonated amines) and water located within the framework. (21) Upon calcination, protons attached to the Co-O-P bridges will balance the negative charge associated with the framework, and this will result in the creation of Brønsted acid centres. Likewise a substitution of Ti(IV) for phosphorous (P(V)), labelled a type II substitution, is another possible mechanisms to generate solid-acid sites in the framework. If a heteroatom can cycle between various oxidation states, for example Co(II/III) or Fe (II/III), then these sites can operate as isolated redox centres for oxidation reactions.(22-25) Simultaneous substitution of both Al(III) and P(V) centres can also occur with Si(IV), particularly in the AFI frameworks(26, 27) via a type-III substitution, to create acid sites. Alternatively, these Al(III) and P(V) sites can be replaced with Co(II/III) and Ti(IV), by using a combination of substitution mechanisms, with the location and proximity of these individual dopants suitably tailored for synergistic catalytic transformations.(22, 28)

The local structure of the active sites in AlPOs determines the nature of the active site. In the case of acidic active centres, the acidity of the framework can greatly vary depending on the bond angles, bond lengths and electrostatic potential around the acid centres.(29) Advances in *in-situ* and operando spectroscopic techniques, as well as computational studies, have enabled the relationship between substitution pathway and nature of the active site to be revealed.(28, 30-32) It is now possible to use that information to design catalytically active centres at the molecular and atomic level with particular local structural environments in order to afford highly active catalysts.

Despite these advantages in tailoring targeted active sites, coupled with the high stability afforded by the microporous framework architecture, they can suffer from poor diffusion due to their interconnecting microporous network. This can have the consequence of reduced substrate scope, inferior turnovers and diminished longevity. In the 1990s, mesoporous materials were developed as an alternative to overcome the mass-transport and diffusion restraints that is prevalent in microporous catalysts. However, despite some successes in the functionalisation of bulky active sites, the overall stability and limitations in scope for a wider integration of transition-metals, restricted their industrial applicability. For example, tetrahedral Ti(IV) ions were incorporated into the framework of Ti-MCM-41 (mesopore aperture 30 Å), but the resulting material did not evoke the same catalytic potential of its microporous analogue, TS-1.(33, 34) This shortcoming inspired a generation to try to combine the advantages of design in a microporous systems, with the improved diffusion offered by ordered mesoporous networks, to create novel hierarchically porous (HP) catalysts (Figure 1).(35-40)

Ryoo and co-workers successfully pioneered a direct hydrothermal assembly approach for the synthesis of dual porosity within zeolites(41) and AlPOs.(42). This process involves utilising an amphiphilic organosilane surfactant that can self-assemble during the hydrothermal synthesis to form micelles, with the concomitant generation of the microporous framework. Upon calcination, the microporous SDA and micelles are removed and a hierarchically porous catalyst was created, which has silanols lining the mesopores (Figure 1). This methodology has proved versatile and has been used to create HP AlPO-n catalysts, with a range of dopants (Co(42), Cr(43), Fe(44), Si(40, 45)), with a large majority focussed on the creation of selective oxidation catalysts. As of yet the relationship between the nature and type of dopant species, which lead to different substitution mechanisms resulting in the creation of diverse active sites for catalysis, has not been fully explored. Herein, we will present the successful synthesis and in-depth characterisation of hierarchically porous Me AlPO-5 with varying metal dopants (Co, Ti and Si). We will further outline how the substitution mechanism alters the nature of the active site and hence their catalytic profiles in the industrially significant Beckmann rearrangement. (46)

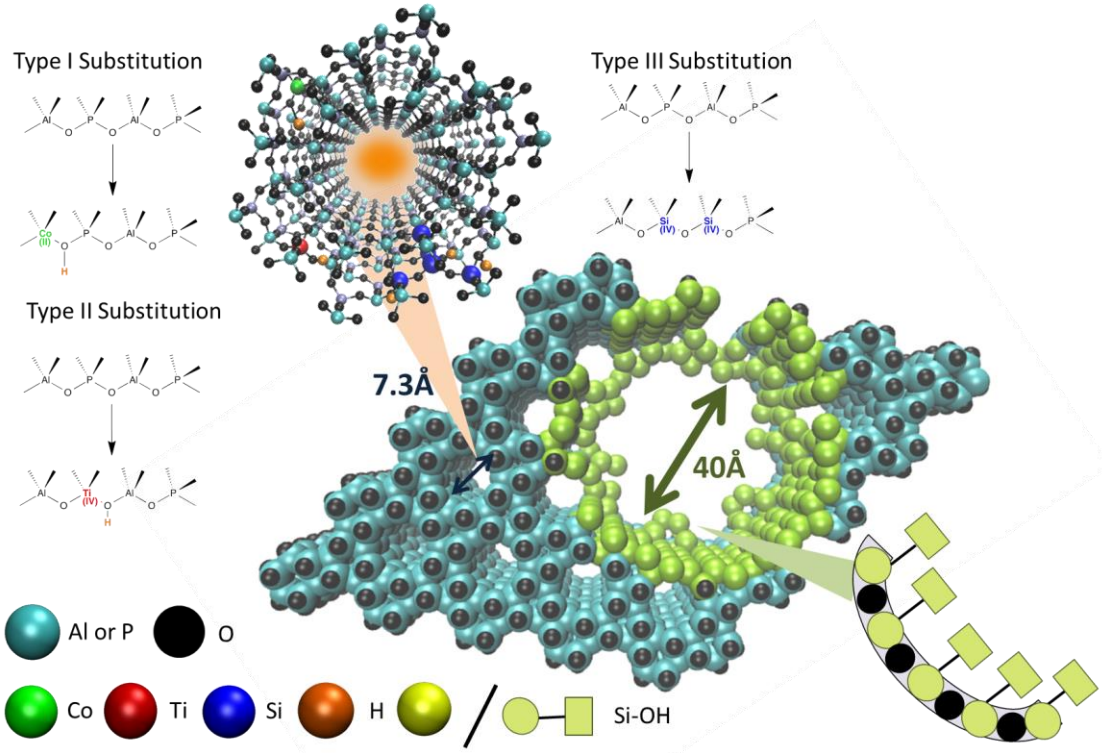

Figure 1: Graphical representation of the HP Me AlPO-5 catalyst and the substitution mechanisms available for the introduction of cobalt, titanium and silicon into the framework.

Experimental

HP Me AlPO-5 Synthesis. The synthetic protocol for the isomorphous substitution of the metals into the hierarchically porous AFI framework is described below. Gel ratios can be found in Table 1.

Aluminium isopropoxide (6.807g, Aldrich) was added to a Teflon beaker with phosphoric acid (2.28ml, 85% in H_2O, Aldrich) and water (10ml), which was vigorously stirred for 1.5 hours until a homogeneous solution was formed. DMOD (dimethyloctadecyl [3(trimethoxylsilyl)propyl] ammonium chloride, 1.2ml, 72% in H2O, Aldrich) was added drop wise, followed immediately by the

gradual addition of triethylamine (3.7ml, Aldrich) and water (20ml). The resulting (dense) solution was stirred for one hour. The metal precursors (in solution) were added drop wise and the gel was stirred for a further 1.5hours. The contents of the gel were transferred to a 23 ml Teflon-lined stainless-steel autoclave, which was allowed to crystallise in a pre-heated, fan-assisted oven (WF-30 Lenton) at 200^{o}C for 24 hours. The solid product from the autoclave was collected via filtration and washed with 500ml of deionised water. The product was left to dry at 80^{o}C overnight. The as-synthesised catalyst was calcined in a tube furnace under a flow of air at 550^{o}C for 16 hours to produce the desired solid.

Table 1: Gel composition and ICP experimental metal loading in the HP Me AlPO-5 catalysts.

Catalyst	Gel Composition	ICP experimental metal loading/wt%
HP Co AlPO-5	1 Al: 1 P: 0.8 SDA: 0.05 DMOD: 50 H_2O: 0.03 Co	Al 23.5%; P 24%; Co 1.5%; Si 1.7%
HP Ti AlPO-5	1 Al: 1 P: 0.8 SDA: 0.05 DMOD: 50 H_2O: 0.03 Ti	Al 19.9%; P 20.6%; Ti 1.1%; Si 1.7%
HP Si AlPO-5	1 Al: 1 P: 0.8 SDA: 0.05 DMOD: 50 H_2O: 0.15 Si	Al 20.6%; P 20.2%; Si 6.63%

Characterisation. Powder X-ray diffraction patterns were collected with a Bruker D2 diffractometer. A micrometrics Gemini 2375 surface area analyser was utilised for BET surface area measurements. FTIR spectra of the pelletized calcined catalysts were recorded using a Nicolet Nexus 870 IR Spectrometer for 128 scans using a cooled MCT detector. The resulting spectra were processed using the GRAMS/Al 9 software (Thermo Scientific). Low temperature CO adsorption involved sequentially adding 0.02cc of CO and, after equilibration for 2 minutes, the spectra was recorded. Collidine adsorption was performed by flowing helium saturated with collidine at 7^{o}C over the sample for 1 hour at 150^{o}C. The stepwise desorption at 150, 300 and 450^{o}C was then performed in flowing helium for 1 hour at each temperature. TPD measurements were collected with a custom-built system using TCD detectors to monitor ammonia concentration. Samples were pretreated by heating at 10 ^{o}C/min to 550 ^{o}C in a 20% O_2/helium mixture for 2 h. The samples were exposed to ammonia and allowed to equilibrate at 150 ^{o}C for 8 h. Desorption was performed in flowing helium at 10 ^{o}C/min to 600 ^{o}C and held for 40 min at 600 °^{o}C. Scanning electron microscopy images were collected with a JSM-5900 LV SEM.

Liquid Phase Beckmann Rearrangement. The Beckmann rearrangement of cyclohexanone oxime to caprolactam was performed in a

glass-reactor under nitrogen. Benzonitrile (20ml) was added to the flask with 0.1g of cyclohexanone oxime (0.88 mmol), 0.1g of chlorobenzene (internal standard) and 0.1g of catalyst (e.g. 0.025 mmol for HP Co AlPO-5). The reaction was performed at 130^{o}C and aliquots were taken frequently in order to monitor the course of the reaction. The solutions were centrifuged and analysed by Perkin Elmer Clarus 480 GC using an Elite-5 column and Flame Ionisation Detector. The products were identified and quantified using chlorobenzene as an internal standard and employing the calibration method. Reproducibility and mass balances were all within acceptable limits.

Structural Characterisation

The HP catalysts were synthesised by utilising a soft-templating bottom up approach. (40) The surfactant, DMOD, was added to the synthesis gel with the microporous structure-directing agent, triethylamine. The Al(III), P(V) and dopant T sites were then able to self assemble around and incorporate the silicon containing surfactant into the microporous framework, thereby creating a truly hierarchically porous framework upon calcination. The calcination process revealed the silanol sites line the mesopores, and the various active sites created by the substitution mechanisms are located within the micropores. Co(II) will be substituted in the framework via type I substitution and Ti (IV) via type II substitution. Both will result in the formation of a charge imbalance that will be balanced by a proton. In the case of the Si(IV) dopant, clustering of this active site often occurs within the AFI framework (as confirmed previously by ^{29}Si NMR(40)), resulting in Al(III) and P(V) being substituted simultaneously via type III substitution.

The effect of the incorporation of the dopant metals (Co, Si and Ti) in the hierarchically porous framework, via the various substitution pathways, was investigated through various characterisation techniques in order to formulate structure property relationships. The structural integrity of the targeted HP Me AlPO-5 was confirmed via powder XRD (Figure 2 A). All catalysts exhibited the intended phase pure AFI framework, despite the metal incorporation. Scanning electron microscopy of the catalysts revealed the expected spherical particles that are usually observed with the AFI framework (Figure 2B-D).(22) The particle sizes were found to be between 5 and 30 μm. Therefore it can be concluded that the dopant metals did not impede the formation of the AFI framework.

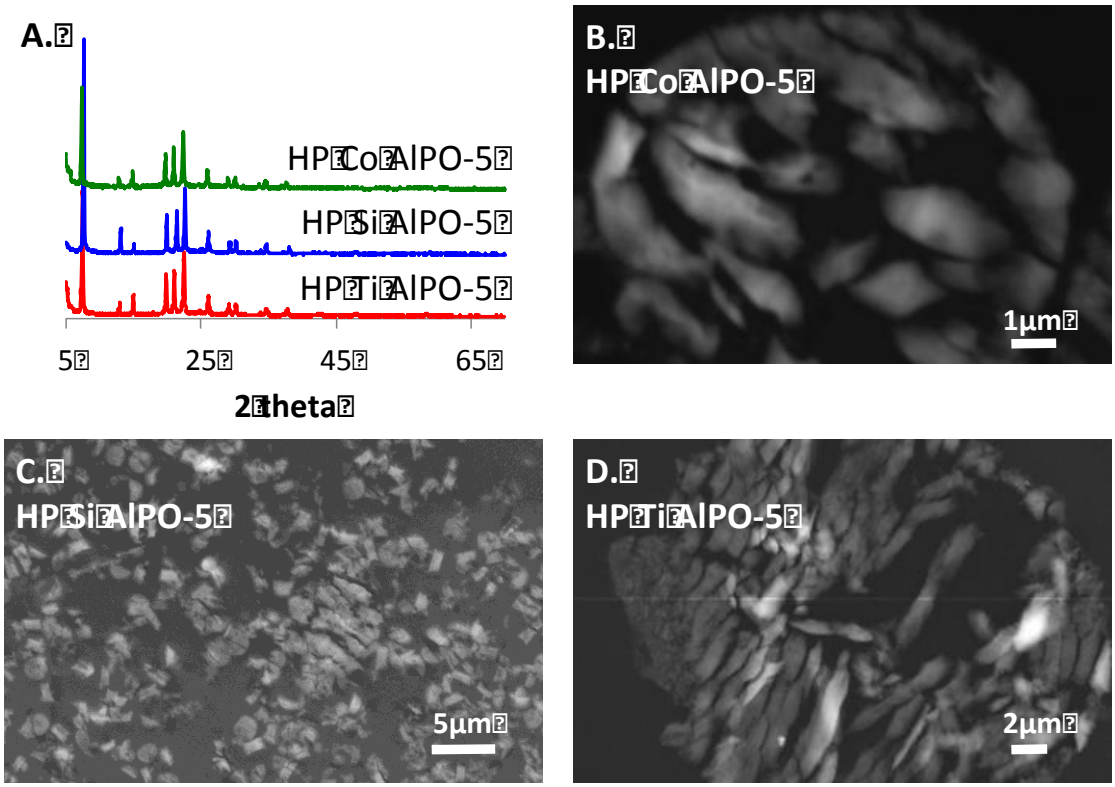

Figure 2: Powder XRD pattern of hierarchically porous Ti AlPO-5 (red), HP Si AlPO-5 (blue) and HP Co AlPO-5 (green) (A). Structural HR SEM evidence substantiating the structure integrity of (B) HP Co AlPO-5, (C) HP Si AlPO-5 and (D) HP Ti AlPO-5.

BET measurements confirmed that the design strategy successfully resulted in the generation of hierarchically porous catalysts regardless of dopant metal and substitution mechanism(Figure 3). All the catalyst exhibited a type IV isotherm, which is indicative of mesoporosity (Figure 3 A). The BJH adsorption pore distribution curves revealed that all the HP catalysts contained mesopores that are approximately 40 Å in diameter (Figure 3B). Encouragingly all the HP catalyst had similar BET surface areas (316-308.1m^2/g) and pore volumes indicating that the inclusion of a transition metal did not obstruct the formation of the HP framework (Table 2).

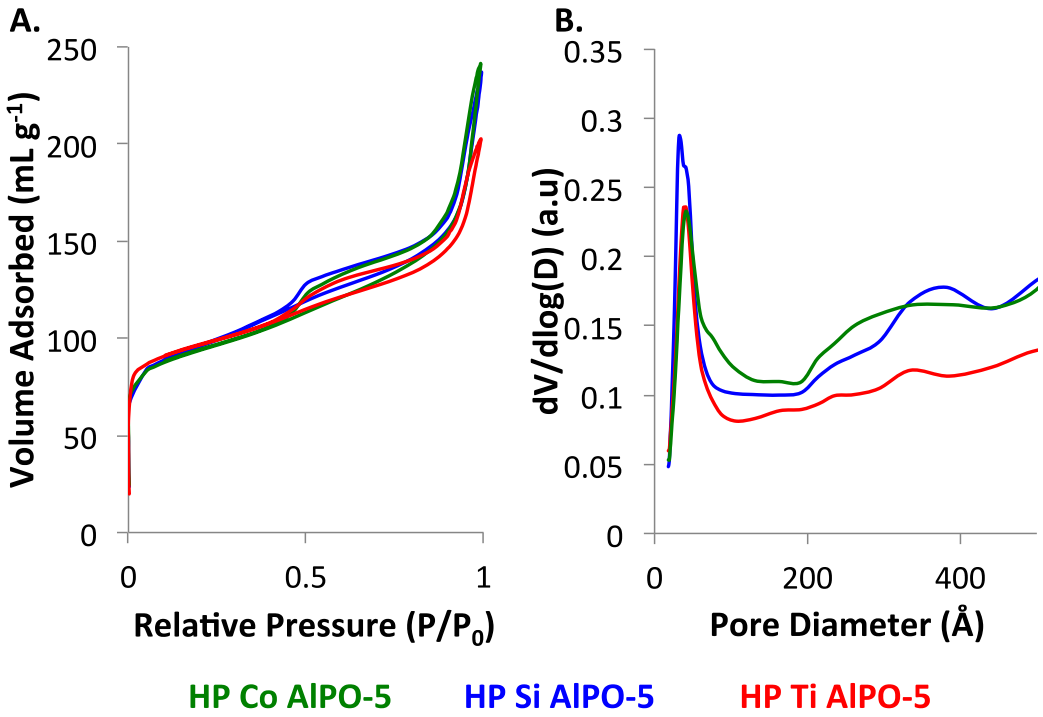

Figure 3: Nitrogen adosrption isotherm (A) and BJH pore distribution curve (B) of HP Co AlPO-5 (green), HP Si AlPO-5 (blue) and HP Ti AlPO-5 (red) providing evidence of the presence of mesopores within the hierahically (dually) porous catalyts.

Table 2: BET parameters of the HP catalysts.

Catalyst	BET surface area (m^2/g)	Mesopore and External Surface Area (m^2/g)	Micropore Surface Area (m^2/g)	Mesopore Volume (cm^3/g)	Micropore Volume (cm^3/g)
HP Co AlPO-5	308.1	111.8	194.4	0.30	0.08
HP Ti AlPO-5	315.0	106.3	205.9	0.23	0.09
HP Si AlPO-5	315.8	121.7	194.1	0.29	0.08

Despite the very different properties of the dopant metals, their inclusion into the HP AlPO-5 framework via either type I, type II or type III substitution mechanism did not greatly impact their structural properties. All catalysts were found to be phase pure and to be formed of spherical particles. The frameworks were also all found to be hierarchically porous in nature with mesopores of 40Å in diameter. In order to evaluate the effect of the dopant substitution on the nature of the active site, a combination of spectroscopic characterisation techniques were utilised.

Nature of the Acid sites

In this study, HP catalysts were designed for the liquid-phase Beckmann rearrangement of cylcohexanone oxime. In order for the catalyst to be effective in this reaction it is imperative that it contains acid sites. Caution should, however, be applied in the design strategy, to take into consideration the strength of these acids sites. If the acid sites are very weak, the reaction will not occur. If the sites are too strong, the basic lactam product will not be able to desorb from the active site, leading to catalyst deactivation and secondary unwanted reactions. In order to characterise the acidity of the HP catalysts, and the effect of the different substitution mechanism on the nature of the active sites, a range of spectroscopic techniques were utilised.

In order to elucidate the nature and strength of the acidic sites FT-IR spectroscopy and temperature programme desorption was utilised. Direct observation of the O-H stretching region of the pre-treated hierarchically porous catalysts revealed that all three catalysts had evidence of bridging Si-OH-Al sites, P-OH/Al-OH defect sites and Si-OH sites, as well as H bonded OH sites to varying degrees (
Figure 4). Interestingly, the HP Si AlPO-5 and HP Co AlPO-5 contained similar levels of bridging Si-OH-Al and Si-OH sites, whereas HP Ti AlPO-5 contained significantly fewer. This could have an impact on the resulting catalytic activity, as both Si-OH sites and bridging Si-OH-Al have been documented to be active sites for the Beckmann rearrangement.(47, 48)

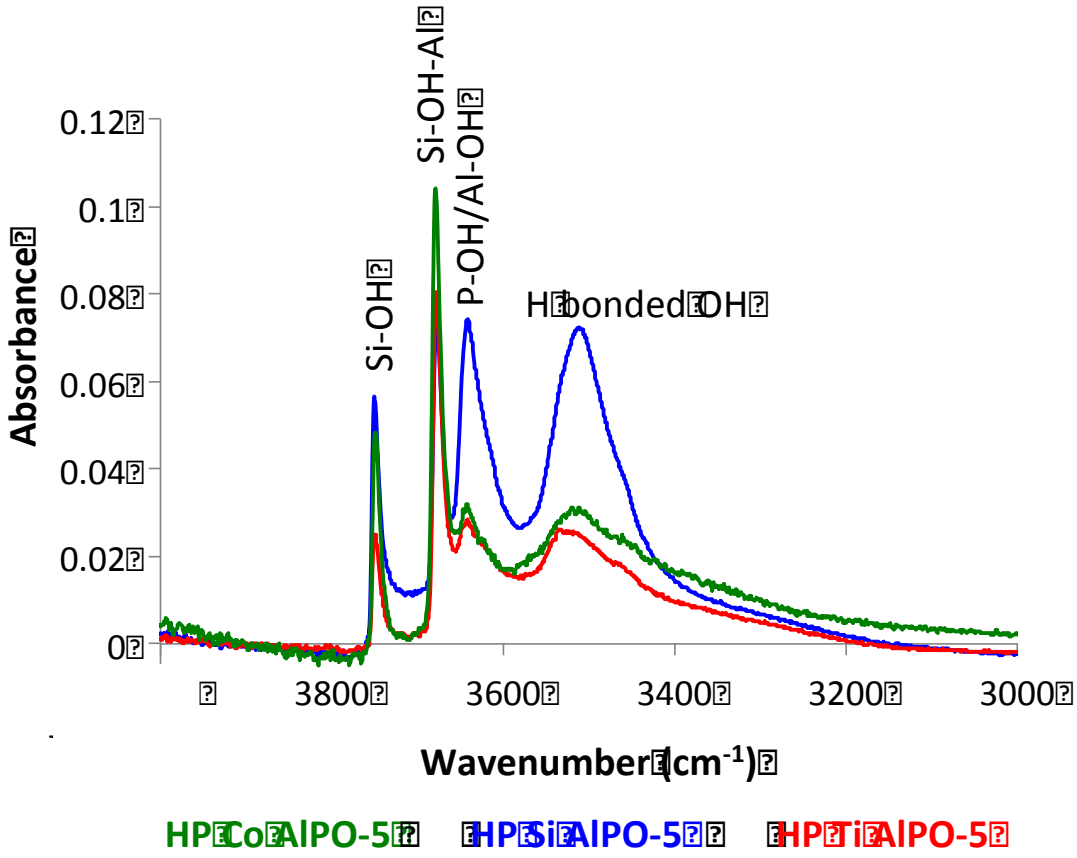

Figure 4: FTIR spectra of the hydroxyl region of calcined HP Co AlPO-5, HP Si AlPO-5 and HP Ti AlPO-5.

The ensuing acid strength of the HP materials will be intimately related to their ensuing catalytic properties. Therefore, the relative quantities of acidity within the HP catalysts was assessed first by temperature programmed desorption with ammonia (Figure 5). The integrated area under the curves can give information regarding the total acidity of the framework and the peak maxima reveals the most prominent acid strength of the catalyst. All three catalysts, irrespective of dopant, have peak maxima of about 280°C. However, HP Co AlPO-5 has a shoulder peak at about 370°C indicating it contains additional stronger acid sites. HP Co AlPO-5 had the largest quantity of acid sites (0.187mmol/g), HP SAPO-5 had intermediate acidity (0.148mmol/g) and HP Ti AlPO-5 had the smallest quantity (0.110mmol/g).

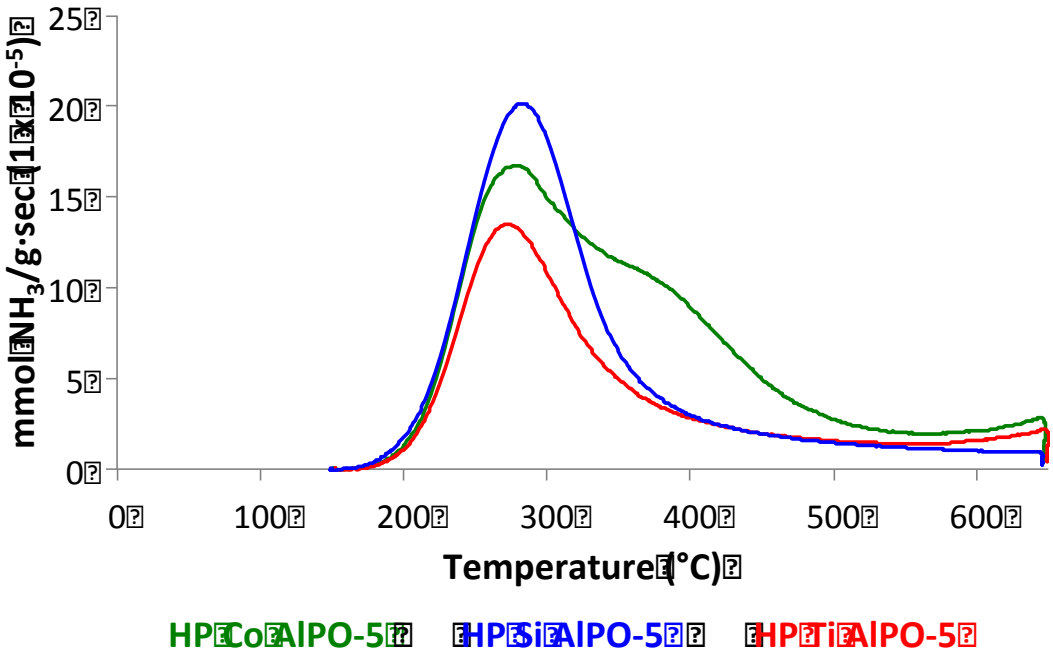

Figure 5: TPD- NH_3 adsorption data of HP Co AlPO-5 (green), HP Si AlPO-5 (blue) and HP Ti AlPO-5 (red).

Temperature programmed desorption does enable the acidity of the catalysts to be assessed indirectly by the strength of the interaction between the adsorbed basic ammonia and the catalyst. However, it is unable to distinguish between Brønsted and Lewis acidic sites and the resolution can be poor. Therefore to gain additional insights into the location and strength of the acid sites within the catalysts, FTIR spectroscopy with probe molecules was utilised. **By using carbon monoxide as a probe molecule with FTIR it is possible to gain an insight into the types of acidity that are present, as well as quantify its strength (**

Figure 6). **The weakly basic CO is able to adsorb and interact with the proton sites within the catalysts, and these OH…CO adducts will result in perturbed O-H and C-O stretches. CO was able to titrate both the Al/P-OH and bridging OH bands in the HP catalysts (**

Figure 6A). The weakly acidic silanol sites, however, only interacted very weakly with the basic CO probe at high CO coverage. The H bonded bands at 3510 cm^{-1} do not interact with CO at the dosing levels indicating that they have much weaker acidity compared to the P-OH and Si-OH-Al groups.

The shifts in frequencies of the bridging OH groups directly relate to the acid site strength. (Table 3). The larger the shift, the greater the acid site strength. All three catalyst had a shift between 273 and 275 cm^{-1}, this shift is quite typical for SAPO catalysts.(26, 40) HP Co AlPO-5 also had an additional stronger acid site, which is associated with a shift of 408cm^{-1}. In the case of the tetravalent dopants, a trend between bond angle and acid site strength in microporous Me AlPO-5 has been observed. The bond angles of the microporous

catalyst increase in the following order Ti-O-Al=119.4< Si-O-Al=132.9, and the acidity of the framework follows the same trend.(49) It is therefore envisaged that the Ti and Si Brønsted acid sites will be found in the micropores of the HP catalyst, hence similar bond angles would be expected. Encouragingly, a similar trend in acidity is observed with the HP Me AlPO-5 catalysts as was observed with the microporous analogues.

Table 3: Position of the maxima of the OH stretching frequency of the Brønsted acid sites and their shifts (ν_{OH}) and quantity of acid sites upon CO adsorption at 100K on HP Co AlPO-5, HP Si AlPO-5 and HP Ti AlPO-5.

Catalyst	**Bridging OH**					**CO Area (AU) (0.18cc add)**
	ν_{OH} (cm^{-1})	$\nu_{OH\text{-}CO}$ (cm^{-1})	ν_{OH} (cm^{-1})	$\nu_{OH\text{-}CO}$ (cm^{-1})	$\Delta\ \nu_{OH}$ (cm^{-1})	
HP Co AlPO-5	3644	3366	278	3236	408	2.082
HP Si AlPO-5	3641	3368	273	N/A	N/A	1.065
HP Ti AlPO-5	3641	3366	275	N/A	N/A	0.586

The C-O stretching region (2200-2100cm^{-1}) (

Figure 6B) revealed absorption at 2170cm^{-1} for all of the HP catalysts indicating the presence of Brønsted acid sites. HP Co AlPO-5 also had significant absorption at 2190cm^{-1}, this band can be attributed to Lewis acidity. Microporous Co AlPO-5 is well documented containing Lewis acid and Brønsted acid centres.(50-52) The nature of bonding between divalent dopants and the neighbouring oxygens is considered to be more ionic in nature than M(IV)-O bonds, hence this explains the Lewis acidity of the Me (II) dopants. (53) (49) HP Ti AlPO-5 also had minimal absorption in this region, where as HP Si AlPO-5 had no evidence of Lewis acidity being present in the catalyst. Deconvolution of the FTIR-CO data revealed the distribution of Lewis and Brønsted acidity within the catalysts (Figure 7). HP Si AlPO-5 was found to have the highest contribution of weak Brønsted acid sites and lowest quantity of Lewis acid sites, whereas HP Co AlPO-5 had the lowest quantity of Brønsted acidity and highest quantity of Lewis acidity. Hence the type of substitution mechanism is very important in determining the type of acidity in the resulting catalyst.

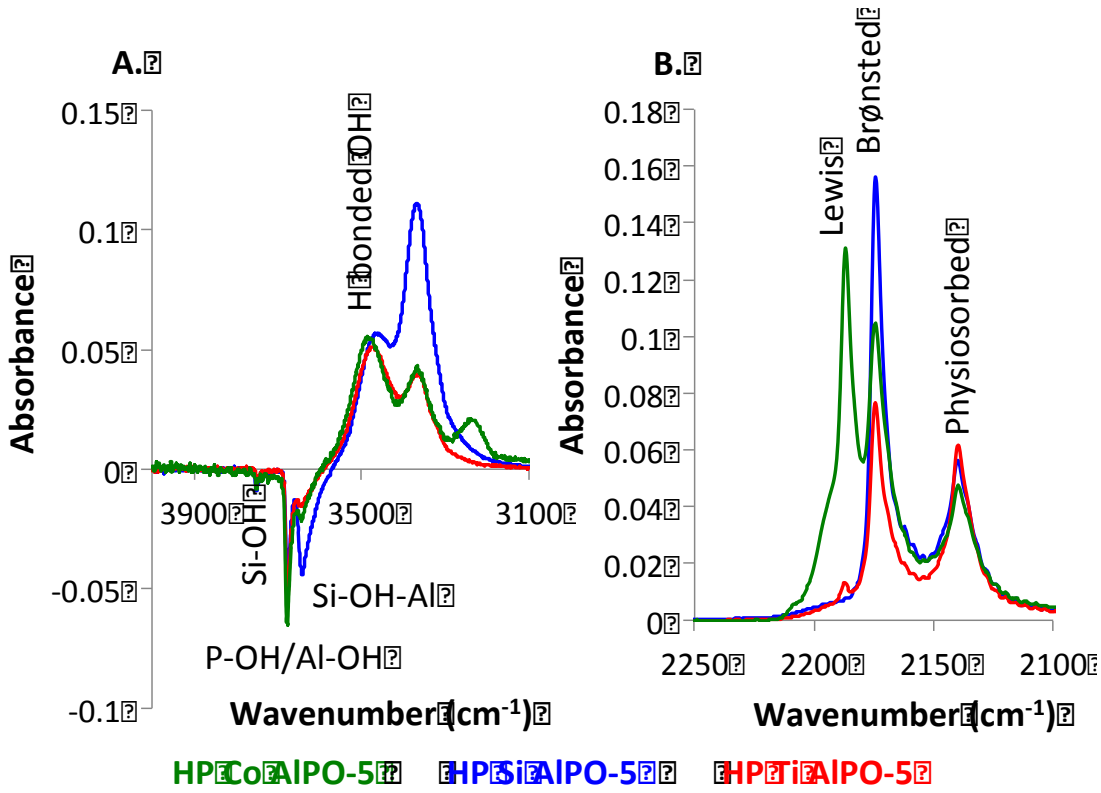

Figure 6: FTIR-spectra of CO adsobred (0.18 cm^3 at 100K) at low temperatures on calcined HP Co AlPO-5 (green), HP Si AlPO-5 (blue) and HP Ti AlPO-5 (red). Hydroxyl region of FTIR-CO (A) and CO region of FTIR-CO (B).

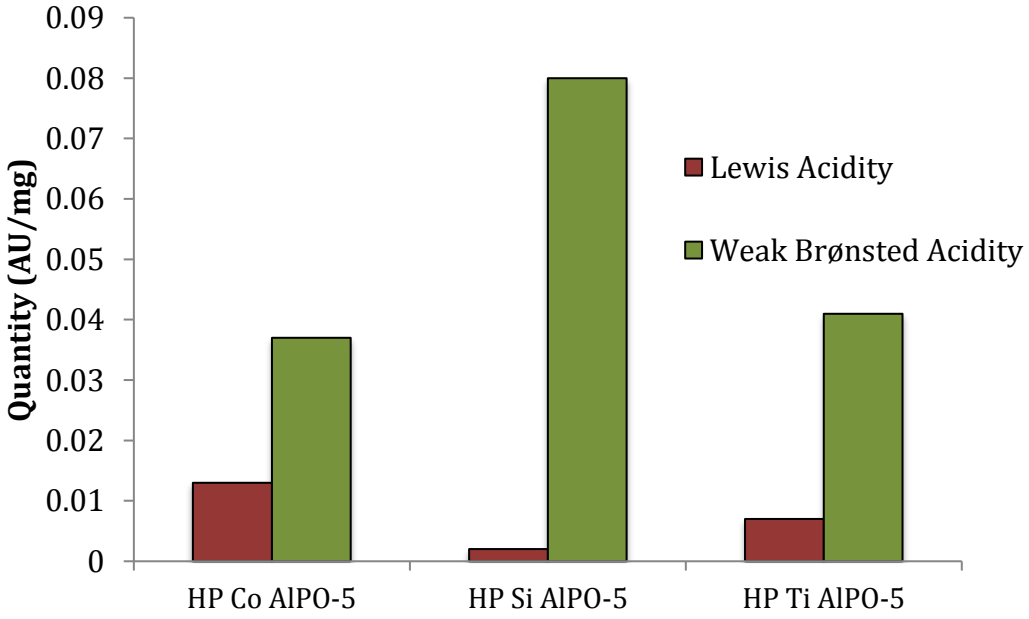

Figure 7: Proportion of Lewis and weak Brønsted acidity of the HP Me AlPO-5 catalysts as determined from deconvoluted FTIR-CO data.

The nature and accessibility of the acid sites within the HP Me AlPO-5 catalyst was further explored by utilising another complementary probe, collidine, 2,3,5-Trimethylpyridine, with FTIR. This molecule was chosen as it has a strong propensity to interact with Brønsted acid sites and it is more bulky than ammonia and CO. Therefore, it would enable the accessibility of the Brønsted acid sites to be investigated. Collidine vapour was first permitted to saturate the pre-treated catalysts, and then the stepwise desorption at 150, 300 and 450°C was recorded. The collidine was observed to interact with all of the hydroxyl groups on all three catalysts. As the temperature was increased collidine was desorbed and very little remained after 450°C. All three catalysts largely consisted of weak to moderate strength acid sites, with HP Co AlPO-5 containing the additional stronger acid sites (Figure 8). These results are very similar to the TPD-NH_3 observations. The relative strength of acid sites is very important within heterogeneous catalysts, as variations in acid-site density and strength favour different reactions. For example, the MTO process favours strong acid sites, whereas the Beckmann rearrangement favours weaker acid sites. The inclusion of the inappropriate strength acid sites within the catalyst can lead to the catalyst being less selective for the reaction.

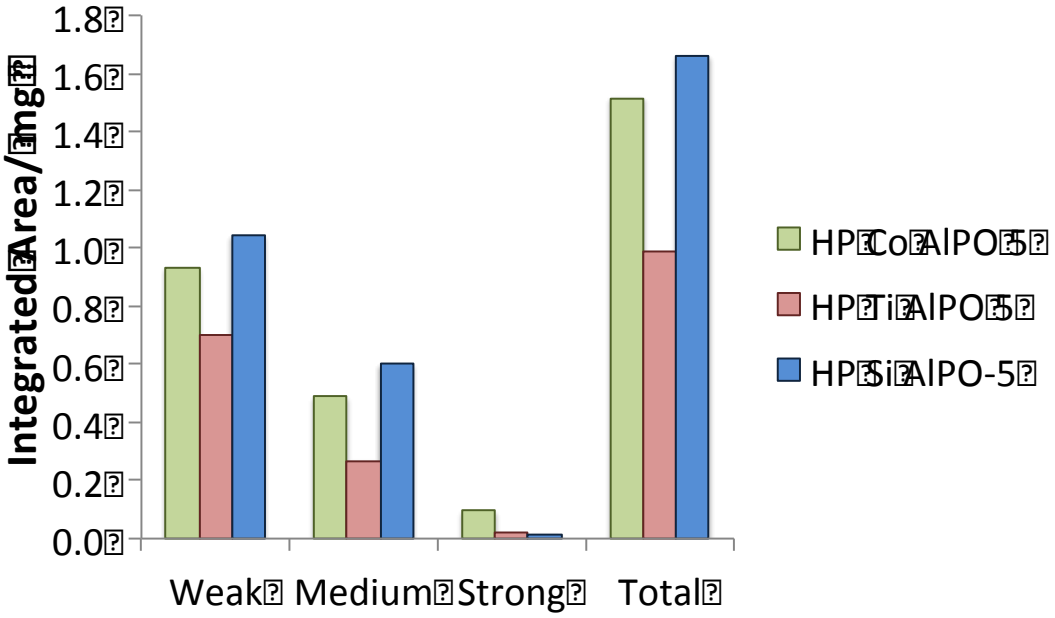

Figure 8: FTIR collidine data for the HP Me AlPO-5 catalysts quantifying the strength of the various Brønsted acid sites within each dopant category.

Influence of substitution pathway on catalytic profile

Regardless of the dopant metal, all the HP Me AlPO-5 catalysts in this study were found to be hierarchically porous in nature and phase pure. They all contain mesopores of approximately 40Å in diameter as well as the microporous

AFI framework. Additionally, by utilising a combination of spectroscopic acid characterisation techniques, the HP Me AlPO-5s have all been found to contain silanol sites as well as the isolated Brønsted acid sites; both are known to be active in the Beckmann rearrangement.(54) Interestingly the type I substituted HP Co AlPO-5 also had a significant quantity of Lewis acidity, type II substituted HP Ti AlPO-5 had minimal Lewis acidity, while HP Si AlPO-5 had no observable Lewis acidity. Given the contrasting nature of the acid active sites found within the HP Me AlPO-5 catalysts, the liquid-phase Beckmann rearrangement was devised as a means to catalytically probe the nature of these sites further.

The Beckmann rearrangement of cyclohexanone oxime is industrially relevant, as it is used to produce 3 million tonnes of ε-caprolactam (the precursor to Nylon-6) every year.(55) It is traditionally carried out in the gas-phase (47, 56-58) (with temperatures in excess of 350 °C), that result in the formation of condensation by-products, that can impede the selectivity of the reaction. Most liquid-phase process with microporous catalysts undergo mass-transfer and diffusion limitations. Mineral acids and oleum (55, 59) have been used as homogeneous catalysts for the liquid-phase Beckmann rearrangement, but these have environmental implications. Hence, by utilising a solid-acid catalyst the process is far more benign and it offers additional advantages from a catalyst recycle perspective.(60-62) The liquid phase Beckmann rearrangement is known to require weak Brønsted acid sites (Figure 9A). (47)The presence of Lewis acid sites is well documented to favour the hydrolysis product cyclohexanone (Figure 9B).(62, 63) The three HP catalysts used in this study possess Brønsted acidity with varying degrees of Lewis acidity. By assessing the performance of these catalysts in this reaction, structure property relationships in the context of substitution mechanisms, can be formulated.

Interestingly, all three HP catalysts were active in the liquid-phase Beckmann rearrangement of cyclohexanone (Figure 9), at temperatures as low as 130 °C. HP Co AlPO-5 had the highest level of conversion at 44% and HP Ti AlPO-5 had the lowest at 30%. Furthermore, the magnitude of catalytic activity can be directly related to the quantity of acid sites, as determined from TPD-NH_3: HP Co AlPO-5 > HP Si AlPO-5 > HP Ti AlPO-5. (Figure 5). Analysis of the selectivity of the catalysts was extremely revealing. The type I substituted HP Co AlPO-5 favoured the formation of the hydrolysis product, cyclohexanone. HP Co AlPO-5 afforded just 47% selectivity to the desired ε-caprolactam, whereas the type II and type III substituted HP Ti AlPO-5 and HP Si AlPO-5 had 100% selectivity to the caprolactam. This can be duly rationalised if the nature and type of acid sites are considered. Type I substitution of cobalt into the HP AlPO-5 framework resulted in the formation of both Lewis acid and Brønsted acid sites (

Figure 6 and Figure 7). The type III substitution of Si into the framework resulted in just Brønsted acidity, while type II substitution resulted in very minimal Lewis acidity. The inclusion of a significant quantity of Lewis acidity resulted in the generation of the appropriate acid site for the unwanted side reaction, the formation of ketone. The ideal active site for the Beckmann rearrangement is a weak Brønsted acid centre, which is present in HP Ti AlPO-5 and HP Si AlPO-5. The spectroscopic revelations from TPD-NH_3, FTIR-CO and FTIR-Collidine further vindicate the structure-property correlations to the dopant substitution mechanism.

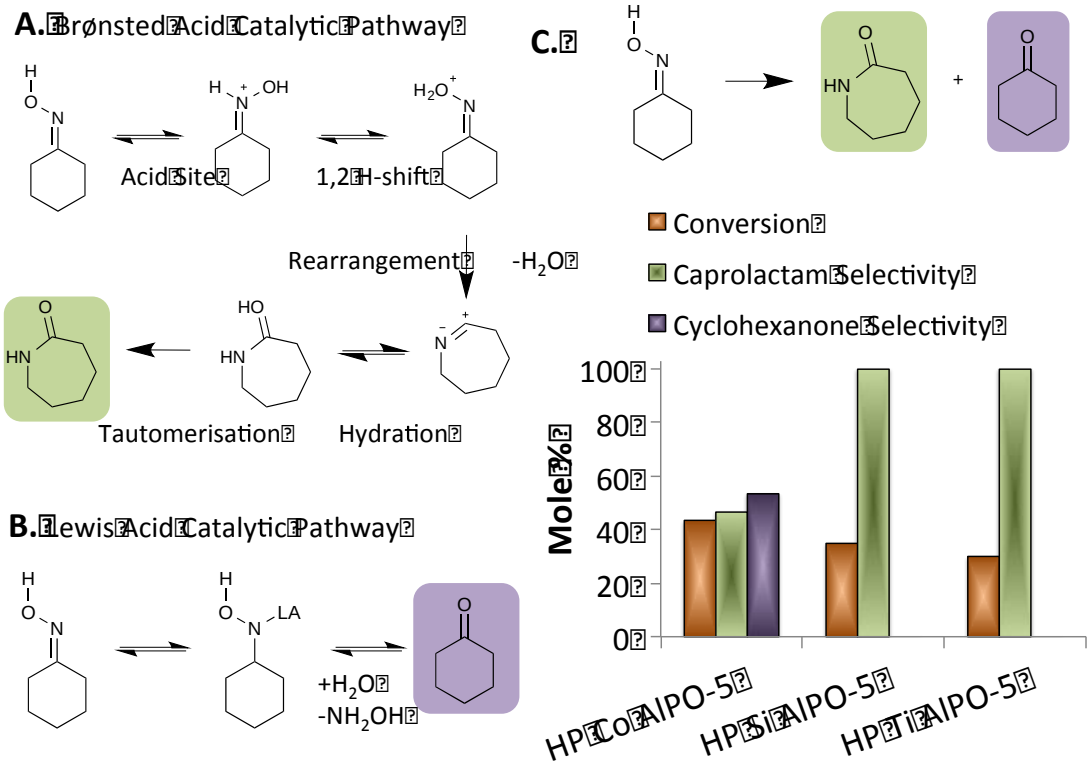

Figure 9: Schematic detailing the mechanistic pathways for the conversion of cyclohexanone oxime to ε-caprolactam using Bronsted acid sites (A) and Lewis acid sites (B). The catalytic activity and selectivity of the HP Me AlPO-5 for the liquid-phase Beckmann rearrangement is shown in (C). Conditions are detailed in the experimental section.

Future Outlooks

Microporous Me AlPOs and SAPOs have been shown by us and others to be highly effective catalysts for a range of selective oxidation and acid-catalysed processes. Careful consideration of framework topology and composition has lead to a new generation of versatile catalysts that can be subtly tailored for an array of catalytic transformations. However, despite these advantages these catalysts do have shortcomings due to their microporous nature. The micropores which house the active sites can be easily blocked, leading to mass-transport and diffusional constraints and be inaccessible to reagents, therefore reducing their activity and applicability for certain reactions. We have shown that by utilising a soft templating technique it is possible to synthesise a range of hierarchically porous AlPO-5 catalysts, with dopants introduced via the three available substitution mechanisms.

Regardless of the dopant species, all the catalysts were found to be phase pure and microporous in nature, although they did have different active sites,

owing to the substitution pathway of the dopants. HP Co AlPO-5 was found to have a considerable Lewis acid nature, whereas HP Si AlPO-5 acid sites were purely Brønsted in nature. These differences in the nature and strength of the acid sites impacted the selectivity of the catalyst, in the liquid phase Beckmann rearrangement. The Lewis acidic HP Co AlPO-5 suffered from poor selectivity, whereas the preferred Brønsted acidic HP Si AlPO-5 was 100% selective to the desired ε-caprolactam product.

These preliminary findings highlight the potential that these hierarchically porous catalysts offer. It can be envisaged that the hierarchically porous catalysts will be able to host a plethora of different types of active sites, found traditionally within the microporous Me AlPOs, for a range of catalytic reactions. These hierarchically porous materials with their dual porosity represent a new class of catalysts that have the potential to build upon the advantages of their microporous counterparts for a range of industrially-significant catalytic transformations.

Data accessibility

The datasets supporting this article have been uploaded as part of the supplementary material.

Competing interests

We have no competing financial interests

Authors' Contributions

SHN carried out the synthesis and catalysis lab work, participated in data analysis, design of the study and compiling the initial draft of the manuscript. WS carried out the HRTEM work and participated in the design of the study. TM carried out the FTIR and TPD lab work and participated in the design of the study. SRB participated in the design of the study and coordinated the FTIR, TPD and HRTEM characterisation. RR conceived the basis and idea behind the project, designed and coordinated the study and finalised the manuscript for submission.

All authors have given their final approval for the publication.

Acknowledgements

We are grateful to Honeywell USA for a PhD studentship to SN and for industrial support.

Funding Statement

RR and SHN kindly thank the UK Catalysis Hub for resources and support provided *via* our membership of the UK Catalysis Hub Consortium and funded by EPSRC *via* grants EP/K014706/1, EP/K014668/1, EP/K014854/1, EP/K014714/1 and EP/M013219/1.

Ethics Statement

Not applicable

References

1. Thomas JM, Raja R, Lewis DW. Single- Site Heterogeneous Catalysts. Angew Chem Int Ed. 2005;44:6456-82.10.1002/anie.200462473
2. Thomas JM, Raja R, Sankar G, Bell RG. Molecular-sieve catalysts for the selective oxidation of linear alkanes by molecular oxygen. Nature. 1999;398:227-30.10.1038/18417
3. Thomas JM, Raja R. Exploiting Nanospace for Asymmetric Catalysis: Confinement of Immobilized, Single-Site Chiral Catalysts Enhances Enantioselectivity. Acc Chem Res. 2008;41(6):708-20.10.1021/ar700217y
4. Thomas JM, Raja R. Catalytically active centres in porous oxides: design and performance of highly selective new catalysts. Chem Commun. 2001:675-87.10.1039/b100369k
5. Newland SH, Xuereb DJ, Gianotti E, Marchese L, Rios R, Raja R. Highly effective design strategy for the heterogenisation of chemo- and enantioselective organocatalysts. Catal Sci Technol. 2015;5:660-5. 10.1039/c4cy00895b
6. Gianotti E, Diaz U, Velty A, Corma A. Designing bifunctional acid-base mesoporous hybrid catalysts for cascade reactions. Catal Sci Technol 2013;3:2677-88.10.1039/c3cy00269a
7. Johnson BFG, Raynor SA, Shephard DS, Mashmeyer T, Thomas J, M;, Sankar G, et al. Superior performance of a chiral catalyst confined within mesoporous silica. Chem Commun. 1999:1167-8.10.1039/A902441G
8. Wilson ST, Lok BM, Messina CA, Cannan TR, Flanigen EM. Aluminophosphate Molecular Sieves: A New Class of Microporous Crystalline Inorganic Solids. J Am Chem Soc. 1982;104:1146-7.10.1021/ja00368a062
9. Guo B, Zhu L, Hu X, Zhang Q, Tong D, Li G, et al. Nature of vanadium species on vanadium silicalite-1 zeolite and their stability in hydroxylation reaction of benzene to phenol. Catal Sci Technol. 2011;1:1060-7.10.1039/c1cy00105a
10. Clerici MG, Bellussi G, Romano U. Synthesis of propylene oxide from propylene and hydrogen peroxide catalyzed by titanium silicate. J Catal. 1991;129:159-67.10.1016/0021-9517(91)90019-Z
11. Gontier S, Tuel A. Liquid Phase Oxidation of Aniline over Various Transition-Metal-Subsituted Molecular Sieves. J Catal 1995;157:124-32.10.1006/jcat.1995.1273

12. Nemeth L, Bare SR. Science and Technology of Framework Metal-Containing Zeotype Catalysts. Adv Catal. 2014;57:1-97.10.1016/B978-0-12-800127-1.00001-1
13. Taramasso M, Perego G, Notari B, inventors. US Pat. 4,410,5011983.
14. Clerici MG, Romano U, inventors. US Pat, 4,824,9761989.
15. Notari B. Microporous crystalline titanium silicates. Adv Catal 1996;41:253-334.10.1016/S0360-0564(08)60042-5
16. Notari B. Titanium Silicate: A New Selective Oxidation Catalyst. Stud Surf Sci Catal. 1991;60:343-52.10.1016/S0167-2991(08)61912-6
17. Jiang T, Wang W, Han B. Catalytic hydroxylation of benzene to phenol with hydrogen peroxide using catalysts based on molecular sieves New J Chem. 2013;37:1654-64.10.1039/c3nj41163j
18. Panov GI, Uriarte AK, Rodkin MA, Sobolev VI. Generation of active oxygen speices on solid surfaces. Opportunity for novel oxidaiton technologies over zeolites. Catal Today. 1998;41:365-85.10.1016/S0920-5861(98)00026-1
19. Li J, Yu J, Xu R. Progress in heteroatom-containing aluminophosphate molecular sieves Proc R Soc A. 2012;468:1955-67.10.1098/rspa.2012.0058
20. Raja R, Potter ME, Newland SH. Predictive design of engineered multifunctional solid catalysts. Chem Commun. 2014;50:5940-57.10.1039/c4cc00834k
21. Feng P, Bu X, Stucky GD. Hydrothermal syntheses and structural characterization of zeolite analogue compounds based on cobalt phosphate. Nature. 1997;388:736-40.10.1038/41937
22. Paterson J, Potter M, Gianotti E, Raja R. Engineering active sites for enhancing synergy in heterogeneous catalytic oxidations. Chem Commun. 2011;47:517-9.10.1039/c0cc02341h
23. Pârvulescu V, Tablet C, Anastasescu C, Su BL. Activity and stability of bimetallic Co (V, Nb, La)-modified MCM-41 catalysts. Catal Today 2004;93-95:307-13.10.1016/j.cattod.2004.06.006
24. Ribera A, Arends IWCE, de Vries S, Pérez-Ramírez J, Sheldon RA. Preparation, Characterization, and Perfomance of FeZSM-5 for the Selective Oxidation of Benzene to Phenol with N2O. J Catal. 195;195:287-97.10.1006/jcat.2000.2994
25. Zhao X, Sun Z, Zhu Z, Li A, Li G, Wang X. Evaluation of Iron-Contaning Aluminophosphate Molecular Sieve Catalysts Prepared by Different Methods for Phenol Hydroxylation. Catal Lett. 2013;143:657-65.10.1007/s10562-013-1027-1
26. Potter ME, Cholerton ME, Kezina J, Bounds R, Carravetta M, Manzoli M, et al. Role of Isolated Acid Sites and Influence of Pore Diameter in the Low-Temperature Dehydration of Ethanol. ACS Catal. 2014;4:4161-9.10.1021/cs501092b
27. Sastre G, Lewis D, W;, Catlow CRA. Modeling of Silicon Substitution in SAPO-5 and SAPO-34 Molecular Sieves. J Phys Chem B. 1997;101(27):5249-62.10.1021/jp963736k
28. Potter ME, Paterson AJ, Mishara B, Kelly SD, Bare SR, Corà F, et al. Spectroscopic and Computational Insights on Catalytic Synergy in Bimetallic Aluminophosphate Catalysts. J Am Chem Soc. 2015;137(26):8534-40.10.1021/jacs.5b03734

29. Pastore HO, Coluccia S, Marchese L. Porous Aluminophosphates: From Moelcular Sieves to Designed Acid Catalysts. Annu Rev Mater Res. 2005;35:351-95.10.1146/annurev.matsci.35.103103.120732
30. Thomas J, M;, Sankar G. The Role of Synchrotron-Based Studies in the Elucidation and Design of Active Sites in Titanium-Silica Epoxidation Catalysts. Acc Chem Res 2001;34:571-81.10.1021/ar010003w
31. Kerssen MM, Sprung C, Whiting GT, Weckhuysen BM. Selective staining of zeolite acidity: Recent progress and future perspectives on fluorescence microscopy. Micro Meso Mater. 2014;189:136-43.10.1016/j.micromeso.2013.10.015
32. Weckhuysen BM. Determing the active site in a catalytic process: Operando spectroscopy is more than a buzzword. Phys Chem Chem Phys. 2003;5:4351-60.10.1039/b309650p
33. Blasco T, Corma A, Navarro MT, Pérez-Pariente J. Synthesis, Characterization, and Catalytic Activity of Ti-MCM-41 Structures. J Catal. 1995;156:65-74.10.1006/jcat.1995.1232
34. Hulea V, Dumitriu E. Styrene oxdiation with H2O2 over Ti-containing molecular sieves with MFI, BEA and MCM-41 topologies. Appl Catal A: Gen. 2004;277:99-106.10.1016/j.apcata.2004.09.001
35. Li K, Valla J, Garcia-Martinez J. Realizing the Commercial Potential of Hierarchical Zeolites: New Opportunitites in Catalytic Cracking. ChemCatChem. 2014;6:46-66.10.1002/cctc.201300345
36. Verboekend D, Pérez-Ramírez J. Design of hierarchical zeolite catalysts by desilication. Catal Sci Technol. 2011;1:879-90.10.1039/c1cy00150g
37. Tzoulaki D, Jentys A, Perez-Ramirez J, Egeblad K, Lercher JA. On the location, strength and accessibility of Bronsted acid sites in hierarchical ZSM-5 particles. Catalysis Today. 2012;198(1):3-11.10.1016/j.cattod.2012.03.078
38. Na K, Choi M, Ryoo R. Recent advances in the synthesis of hierarchically nanoporous zeolites. Micro Meso Mater. 2013;166:3-19.10.1016/j.micromeso.2012.03.054
39. Parlett C, M, A;, Wilson K, Lee A. Hierarchical porous matierals: catalytic applications. Chem Soc Rev. 2013;42:3876-93.10.1039/c2cs35378d
40. Newland SH, Sinkler W, Mezza T, Bare SR, Carravetta M, Haies IM, et al. Expanding Beyond the Micropore: Active-Site Engineering in Hierarchical Architectures for Beckmann Rearrangement. ACS Catal 2015;5:6587-93. 10.1021/acscatal.5b01595
41. Choi M, Cho HS, Srivastava R, Venkatesan C, Choi D-H, Ryoo R. Amphiphilic organosilane-directed synthesis of crystalline zeolite with tunable mesoporosity. Nature Materials. 2006;5:718-23.10.1038/nmat1705
42. Choi M, Srivastava R, Ryoo R. Organosilane surfactant-directed synthesis of mesoporous aluminophosphates constructed with crystalline microporous frameworks. Chem Commun. 2006:4380-2.10.1039/b612265e
43. Kim J, Bhattacharjee S, Jeong K, Jeong S, Choi M, Ryoo R, et al. CrAPO-5 catalysts having a hierarchical pore structure for the selective oxidation of tetralin to 1-tetralone. New J Chem. 2010;34:2971-8.10.1039/c0nj00493f
44. Wang F, Liang L, Ma J, Shi L, Sun J. Compressed CO2 Accelerated the Synthesis of Mesoporous Heteroatom-Substituted Aluminophosphates for Enhanced Catalytic Activity. Eur J Inorg Chem. 2014:2934-40.10.1002/ejic.201402060

45. Sun Q, Wang N, Xi D, Yang M, Yu J. Organosilane surfactant-directed synthesis of hierarchical porous SAPO-34 catalysts with excellent MTO performance. Chem Commun. 2014;50:6502-5.10.1039/c4cc02050b
46. Icihashi H, Sato H. The development of new heterogeneous catalytic processes for the production of ε-caprolactam. Appl Catal A: Gen. 2001;221:359-66.10.1016/S0926-860X(01)00887-0
47. Izumi Y, Ichihashi H, Shimazu Y, Kitamura M, Sato H. Development and Industrialization of the Vapor-Phase Beckmann Rearragemnet Process Bull Chem Soc Jpn. 2007;80(7):1280-7.10.1246/bcsj.80.1280
48. Fernandes A, Marinas A, Blasco T, Fornes V, Corma A. Insight into the active sites for the Beckmann rearrangement on porous solids by in situ infrared spectroscopy. J Catal. 2006;243:270-7.10.1016/j.jcat.2006.06.029
49. Elanany M, Vercauteren DP, Kubo M, Miyamoto A. The acidic properties of H-MeAlPO-5 (Me=Si, Ti, or Zr): A periodic density functional study. J Mol Catal A-Chem. 2006;248:181-4.10.1016/j.molcata.2005.12.026
50. Barrett PA, Sankar G, Catlow CRA, Thomas J, M;. X-ray Absorption Spectroscopic Study of Brønsted, Lewis, and Redox Centers in Cobalt-Substituted Aluminum Phosphate Catalysts. J Am Chem Soc. 1996;100:8977-85.10.1021/jp953034f
51. Beale AM, Sankar G, Catlow CRA, Anderson PA, Green TL. Towards an understanding of the oxidation state of cobalt and manganese ions in framework substituted microporous aluminophosphate redox catalysts: An electron paramagnetic resonance and X-ray absorption spectroscopy investigation. Phys Chem Chem Phys. 2005;7:1856-60.10.1039/B415570J
52. Leithall RM, Shetti VN, Maurelli S, Chiesa M, Gianotti E, Raja R. Toward understanding the catalytic synergy in the design of bimetallic Molecular Sieves for Selective Aerobic Oxidations. J Am Chem Soc. 2013;135:2915-8.10.1021/ja3119064
53. Saadoune I, Corà F, Catlow CRA. Computational Study of the Structural and Electronic Properties of Dopant Ions in Microporous AlPOs. 1. Acid Catalytic Activity of Divalent Metal Ions. J Phys Chem B. 2003;107(13):3003-11.10.1021/jp027285h
54. Marthala VRR, Jiang Y, Huang J, Wang W, Gläser R, Hunger M. Beckmann Rearrangement of 15 N-Cyclohexanone Oxime on Zeolites Silicalite-1, H-ZSM-5, and H-[B]ZSM-5 Studied by Solid-State NMR spectroscopy. J Am Chem Soc. 2006;128:14812-3.10.1021/ja066392c
55. L. Crescentini WBF. Caprolactam. Kirk-Othmer Encyclopedia of Chemical Technology. 2000.10.1002/0471238961.0301161806091908.a01
56. Kumar R, Chowdhury B. Comprehensive Study for Vapor Phase Beckmann Rearrangement Reaction over Zeolite Systems. Ind Eng Chem Res. 2014;53:16587-99.10.1021/ie503170n
57. Heitmann GP, Dahlhoff G, Holderich WF. Catalytically Active Sites for the Beckmann Rearrangement of Cyclohexanone Oxime to E-Caprolactam. Journal of Catalysis. 1999;186:12-9.10.1006/jcat.1999.2552
58. Icihashi H, Kitamura M. Some aspects of the vapor phase Beckmann rearrangement for the production of caprolactam over high silica MFI zeolites. Catalysis Today. 2002;73:23-8.10.1016/S0920-5861(01)00514-4

59. Bellussi G, Perego C. Industrial catalytic aspects of the synthesis of monomers for nylons production CATTECH. 2000;4(1):4-16.10.1023/A:1011905009608
60. Camblor MA, Corma A, García H, Semmer-Herlédan V, Valencia S. Active Sites for the Liquid-Phase Beckmann Rearrangment of Cylcohexanone, Acetophenone and Cylcododecanone Oximes, Catalyzed by Beta Zeolites. J Catal. 1998;177:267-72.10.1006/jcat.1998.2110
61. Opanasenko M, Shamzhy M, Lamač M, Čejka J. The effect of substrate size in the Beckmann rearrangement: MOF vs. Zeolites. Catal Today. 2013:94-100.10.1016/j.cattod.2012.09.008
62. Ngamcharussrivichai C, Wu P, Tatsumi T. Active and selective catalyst for liquid phase Beckmann rearrangment of cyclohexanone oxime. J Catal. 2005;235:139-49.10.1016/j.jcat.2005.07.020
63. Ngamcharussrivichai C, Wu P, Tatsumi T. Selective Production of caprolactam via Liquid phase Beckann Rearrangement of Cyclohexanone Oxime over HUSY Catalyst. Chem Lett. 2004;33(10):1288-9.10.1246/cl.2004.1288

Figure and Table Captions

Figure 1	Graphical representation of the HP Me AlPO-5 catalyst and the substitution mechanisms available for the introduction of cobalt, titanium and silicon into the framework.
Figure 2	Powder XRD pattern of hierarchically porous Ti AlPO-5 (red), HP Si AlPO-5 (blue) and HP Co AlPO-5 (green) (A). Structural HR SEM evidence substantiating the structure integrity of (B) HP Co AlPO-5, (C) HP Si AlPO-5 and (D) HP Ti AlPO-5.
Figure 3	Nitrogen adosrption isotherm (A) and BJH pore distribution curve (B) of HP Co AlPO-5 (green), HP Si AlPO-5 (blue) and HP Ti AlPO-5 (red) providing evidence of the presence of mesopores within the hierahically (dually) porous catalyts.
Figure 4	FTIR spectra of the hydroxyl region of calcined HP Co AlPO-5, HP Si AlPO-5 and HP Ti AlPO-5.
Figure 5	TPD- NH_3 adsorption data of HP Co AlPO-5 (green), HP Si AlPO-5 (blue) and HP Ti AlPO-5 (red).
Figure 6	FTIR-spectra of CO adsobred (0.18 cm^3 at 100K) at low temperatures on calcined HP Co AlPO-5 (green), HP Si AlPO-5 (blue) and HP Ti AlPO-5 (red). Hydroxyl region of FTIR-CO (A) and CO region of FTIR-CO (B).
Figure 7	Proportion of Lewis and weak Brønsted acidity of the HP Me AlPO-5 catalysts as determined from deconvoluted FTIR-CO data.
Figure 8	FTIR collidine data for the HP Me AlPO-5 catalysts quantifying the strength of the various Brønsted acid sites within each dopant category.
Figure 9	Schematic detailing the mechanistic pathways for the conversion of cyclohexanone oxime to ε-caprolactam using Bronsted acid sites (A) and Lewis acid sites (B). The catalytic activity and selectivity of the HP Me AlPO-5 for the liquid-phase Beckmann rearrangement is shown in (C). Conditions are detailed in the experimental section.
Table 1	Gel composition and ICP experimental metal loading in the HP Me AlPO-5 catalysts.
Table 2	BET parameters of the HP catalysts.
Table 3	Position of the maxima of the OH stretching frequency of the Brønsted acid sites and their shifts (ν_{OH}) and quantity of acid sites upon CO adsorption at 100K on HP Co AlPO-5, HP Si AlPO-5 and HP Ti AlPO-5.